Radiating encouragement: further investigation into the application of gamma ray spectroscopy for archaeological prospection at the Roman town of Silchester

Archaeological Prospection

WILEY

RESEARCH ARTICLE OPEN ACCESS

Radiating Encouragement: Further Investigation Into the Application of Gamma Ray Spectroscopy for Archaeological Prospection at the Roman Town of Silchester

Victoria Robinson[1,2] | Stuart Black[1] | Robert Fry[1] | Helen Beddow[2] | Robert Clark[2] | Mike Fulford[1]

[1]School of Archaeology, Geography and Environmental Science, University of Reading, Reading, UK | [2]Nuvia Limited, Warrington, UK

Correspondence: Victoria Robinson (v.a.robinson@pgr.reading.ac.uk)

Received: 15 December 2023 | **Revised:** 17 May 2024 | **Accepted:** 28 June 2024

Funding: The authors received no specific funding for this work.

Keywords: archaeological survey | gamma ray surveying | gamma spectrometry | natural radioactivity | Nuvia Groundhog® | Silchester

ABSTRACT

This study builds on a preliminary investigation into the efficacy of gamma radiation surveying as a complementary tool for archaeological prospection. Improved surveying and data processing methods were implemented, including the use of a vehicle-mounted Groundhog surveying system, use of alternative software tools and examination of the impacts of individual radionuclides. The study focuses on a range of targets within *Insulae* VII, XXXV and XXXIII in Silchester Roman town, Hampshire. Targets of interest included a polygonal temple, a house, ditches (including an Iron Age defensive ditch) and several Roman roads. While the survey revealed no measurable differences in the gamma radionuclide content of less substantial structures (such as the temple and house) and the surrounding soil, it successfully delineated major structures. The Roman roads, Iron Age defensive ditch and potentially an indication of a historic field boundary not present in modern records were clearly visible in the generated visualisations. The roads and field boundary appear as distinct linear features of depleted radioactivity. The location of the Iron Age ditch correlates with an area of elevated radioactivity. Notably, the technique not only successfully identified archaeological features but was also able to indicate differences in the properties of similar targets such as variations in road thickness. Further, the gamma radiation data indicates variations in the local geology attributable to historic changes in land use and geochemical composition. This latest study corroborates the findings of the preliminary investigation, demonstrating replicability, scalability and ability to enhance output data quality. Further research, including sampling and non-destructive analysis of materials from the site, is needed to better explain observed results.

1 | Introduction

Multiple geophysical survey methods have been applied on a global scale as a non-destructive method of identifying and analysing features of archaeological interest for over 70 years (Cuenca-Garcia 2018; Jordan 2009; Wynn 1986). As noted by Jordan (2009), an extensive amount of data has been accrued over this period, demonstrating the successful application of these techniques in supporting archaeological investigations. However, the effectiveness of each method is dependent on the ability to measure clear differences in the physical properties of potential targets and surrounding substrate and susceptibility to interference from modern features (Gaffney and Gater 2011; Milsom and Eriksen 2011; Ruffell and McKinley 2008). Selection of an optimal geophysical technique most likely to yield significant contrasts must therefore be managed on a site-by-site basis. Consideration must be given to the physical characteristics of anticipated targets, the surrounding substrate, target size and presence of modern features that could cause interference (Gaffney and Gater 2011; Ruffell and McKinley 2008).

To improve data fidelity, multiple geophysical survey methods measuring different physical properties, and with different susceptibilities, can be applied. Multiple studies demonstrating the effectiveness of using complementary geophysical methods for the prospection and mapping of archaeological sites are available in the published literature. Key benefits associated with the application of complementary geophysical techniques at a site include improving the accuracy of data interpretation and increasing the amount of data that can be retrieved to characterise a site beyond merely establishing the presence and position of archaeological features. This first point is exemplified in a study by Cuenca-Garcia (2018). Here, multiple geophysical techniques were consistently applied to three contrasting sites of archaeological interest across Scotland. Techniques included fluxgate gradiometer, electromagnetic induction, ground-penetrating radar (GPR) and earth resistance surveys (Cuenca-Garcia 2018). Geochemical analysis of soil samples taken from each site was also undertaken to aid geophysical data interpretation (Cuenca-Garcia 2018). The selected sites contained known targets including a Viking Longhouse, Iron Age ditches and Neolithic/Bronze Age closures. The findings from the study highlighted the benefits of implementing complementary techniques. This is best demonstrated in data from the survey of the Viking Longhouse. The Fluxgate Gradiometer survey was unable to detect the target through the deep windblown sands but was able to detect midden deposits that may have otherwise been missed (Cuenca-Garcia 2018)—a false negative conclusion. In contrast, the GPR and electromagnetic methods were capable of measuring the contrast between the longhouse and surrounding substrate (Cuenca-Garcia 2018). The study highlights the value of such an approach in regions with more challenging geologies for archaeological prospection and in particular those with significant heterogeneity in the soil overburden which can have the effect of shielding responses or creating noise in the output data.

Indeed, the author notes that in areas where significant variability exists, 'surveys based on a single technique … have a high chance of being disappointing …' (Cuenca-Garcia 2018, 70). A later paper by Porcelli et al. (2020) further highlights the importance of utilising multiple datasets to aid interpretation. Within this paper, Porcelli et al. (2020) refers to a GPR survey of Tutankhamun's tomb, undertaken to confirm an earlier theory that it may be part of a larger tomb infrastructure belonging to Queen Nefertiti. This preliminary GPR survey appeared to confirm this theory, with the findings published as the 'discovery of the century' (Porcelli et al. 2020). However, two subsequent GPR surveys covering the same area, including one undertaken by the original authors, showed that this original conclusion was incorrect and that there were no further features of interest (Porcelli et al. 2020)—a false positive result. This second paper highlights the potential vulnerability of using a single technique and how even different datasets using the same technique can lead to conflicting conclusions.

A study by Simon et al. (2015) highlights the value of integrating different geophysical techniques to improve site characterisation, recognising that a single technique will only be able to generate data on one specific parameter of the site. In this study, the authors applied a combination of geophysical techniques to investigate a Neolithic site in Thessaly, Greece. Techniques gainfully employed included magnetic surveys, electrical tomography and GPR (Simon et al. 2015). The combination of techniques yielded data with greater interpretive value. Useful insights into the presence and location of Neolithic structures, depth profiles of these features and indications of the geomorphology and sediment diversity of the area were provided (Simon et al. 2015). Further, the techniques applied facilitated a proportionate approach to surveying and the ability to gain the most amount of information possible within resource constraints. Magnetic and electrical methods enabled the efficient and effective surveying of a substantial area at a useful resolution (Simon et al. 2015). GPR, a higher resolution technique, could then be applied to much smaller areas, targeting features most likely to benefit from this higher resolution (Simon et al. 2015).

In summary, the application of multiple geophysical techniques in archaeological prospection follows a philosophy similar to that of James Lovelock's insightful Gaia theory; that when these different complex techniques are applied cooperatively, the value of the combined data should be greater 'than the sum of its parts' (Lovelock 2000). Building on this philosophy, the authors of this paper aim to assess an alternative nonintrusive survey method's effectiveness in archaeological prospection and its ability to contribute to this multitechnique approach. Specifically, the use of portable gamma radiation systems to measure any contrasts in concentrations of naturally occurring radioactivity in archaeological targets and the surrounding substrate. If successful, the use of gamma surveying methods could add to the existing 'toolbox' of nonintrusive archaeological prospection methods and may even facilitate improved interpretation of acquired data.

This research is the first reporting of a vehicle-mounted gamma radiation survey conducted at an archaeological site, for the purpose of prospection, available within the published literature. Our study successfully demonstrates the repeatability and scalability of the method, as well as an ability to apply multiple processing methods to generate high quality visual outputs that are novel, and that show significant promise for archaeological and land-use investigations.

2 | Building on a Preliminary Investigation at Silchester

Following an earlier study, the authors published findings from a preliminary investigation exploring the efficacy of using gamma radiation surveying methods to support the identification of buried archaeological features (Robinson et al. 2022). This approach is based on the principle that naturally occurring radioactive material is ubiquitous in the environment (IAEA 2023) and that human activity can cause measurable changes in the concentrations of this radioactivity. This includes, for example, importing and depositing (construction) materials from other locations, using clays which are naturally rich in naturally occurring radionuclides to make bricks (Aliyev 2004; IAEA 2003) and other industrial activities. The study focussed on targets within Silchester Roman Town. This location was selected due to the extensive geophysical and archaeological data available for the site

(Creighton and Fry 2016; Fulford 2021). This provided a valuable opportunity to compare gamma surveying data against this existing and well-understood information.

In the preliminary study (Robinson et al. 2022), gamma radiation surveys were undertaken using a hand-held gamma surveying system in both a collimated and uncollimated configuration to target four small areas across the site. Each contained a different target type. The system used was a Groundhog® Fusion system, developed, owned and operated by Nuvia Limited. The Groundhog® Fusion system (subsequently referred to here as Groundhog®) is part of a family of rugged, portable gamma radiation detection systems with spectrometric capability. The key components of Groundhog® used for this study are presented in Section 4. The system can be deployed in various configurations including collimated, uncollimated, vehicle mounted (using a bank of gamma detectors) or hand-held (single gamma detector). Groundhog® systems are traditionally used in the nuclear industry for mapping out anthropogenic radioactive contamination in the environment.

Results using a hand-held gamma detector from this earlier investigation at Silchester showed varying results. Gamma radiation data from two of the areas: an 'urban' site from the centre of the Roman Town and an area containing cremations/inhumations from just outside the Late Roman Town walls, failed to distinguish any archaeological features (Robinson et al. 2022). However, the other two sites, a temple area in the east side of the site and an industrial area in nearby Little London, yielded positive results. Here, the Groundhog® system was able to identify man-made features (both archaeological and more modern) that were also visible within extant fluxgate gradiometer and GPR data. Features identified included a Temenos wall/ditch bounding a Roman temple and an infilled clay pit (Robinson et al. 2022). The results suggested that gamma radiation surveys could be used to support the identification of some buried archaeological features and could add value to a multi-method geophysical approach to a site's identification and interpretation. Completion of this pilot study highlighted a number of opportunities for potentially improving the quality and efficiency of survey outputs. This included improving the scalability of the technique by using Nuvia's vehicle-mounted Groundhog® system and applying different data processing methods. This paper presents the results of work testing these variables.

2.1 | Aspects for Further Investigation

Completion of the first set of gamma surveys highlighted several opportunities for further work to test:

- Whether the findings from the first study could be replicated for other analogous targets,
- Whether the technique could be scaled up to cover a larger area within a similar period of time and
- Methods for improving the quality of processed data used for interpretation.

Two subsequent surveys were therefore undertaken at a different location within Silchester's boundary walls. The new location offered analogous targets, including the Roman road infrastructure, a 16-sided temple structure and a major defensive Iron Age Ditch to test replication. Scalability was tested through the deployment of the vehicle-mounted Groundhog® system, which is capable of operating three gamma detector units simultaneously and, using a traversing speed of ~1 m/s, is able to cover approximately 1.4–2 ha/day. The collected data for this paper was processed using Geoplot 4 (Geoscan Research), enabling further experimentation with data processing. Finally, data from the two surveys were normalised with the intent of integrating the two datasets.

3 | Current Study Site and Existing Data

The study site is situated within the Roman Town of Silchester (Calleva Atrebatum) (Figure 1). The town is located approximately 2 km to the west of the current day village of Silchester, Hampshire, in south-east England. The site has a long history of occupation, dating back to the Iron Age (Fulford 2021). Indeed, one of the targets selected for this study is an Iron Age ditch that formed part of a large defensive enclosure, encompassing an area of ~38 ha (Fulford 2021). The positioning of the later Roman town broadly aligns with this enclosure (Fulford 2021). The Roman town of Silchester hosted various buildings and supporting infrastructure, from domestic dwellings to workshops, shops, temples and road networks (Creighton and Fry 2016; Fulford 2021). The roads divided the town into *insulae*, each generally containing a mixture of building types. It was this diversity of target type, combined with the extensive geophysical and archaeological data already available for the site that cemented Silchester as an optimal case study for this research project. These data have been acquired from over 150 years of systematic excavations at the site, starting principally with Reverend James Joyce in the 1860s (Creighton and Fry 2016) and decades of geophysical survey initiated in the 1950s (Creighton and Fry 2016).

The targets selected for this study are located across *Insulae* VII and XXXV to the west and *Insulae* XXXIII and XXXII to the east.

3.1 | *Insulae* VII and XXXV

The first survey location (Area 'A'), outlined in red in Figure 2, is a 0.6 ha area spanning *Insulae* VII and XXXV and contains three targets of interest (Figure 2). The first target is an anomaly broadly circular in shape, identified as a temple of stone construction, including ironstone quoins (Fulford 2021; Ward 1911). This feature comprises two concentric shapes: the outer being a 16-sided polygonal wall and an inner circular structure with a total maximum diameter of ~20 m (Creighton and Fry 2016). Although the foundations of this temple have previously been described as 'slight' (Creighton and Fry 2016), they produce a clear circular anomaly in the fluxgate gradiometer (Figure 2) and GPR data. The latter suggesting a depth of 1.57 and 0.23 m below the soil surface (Linford, Linford, and Payne 2019). It was therefore hoped that the structure would be substantial enough to support detection of a contrast in naturally occurring radioactive material relative to the surrounding substrate. In addition to the temple, there is '*Insula* VII House 4', an eight-roomed house (Creighton and Fry 2016),

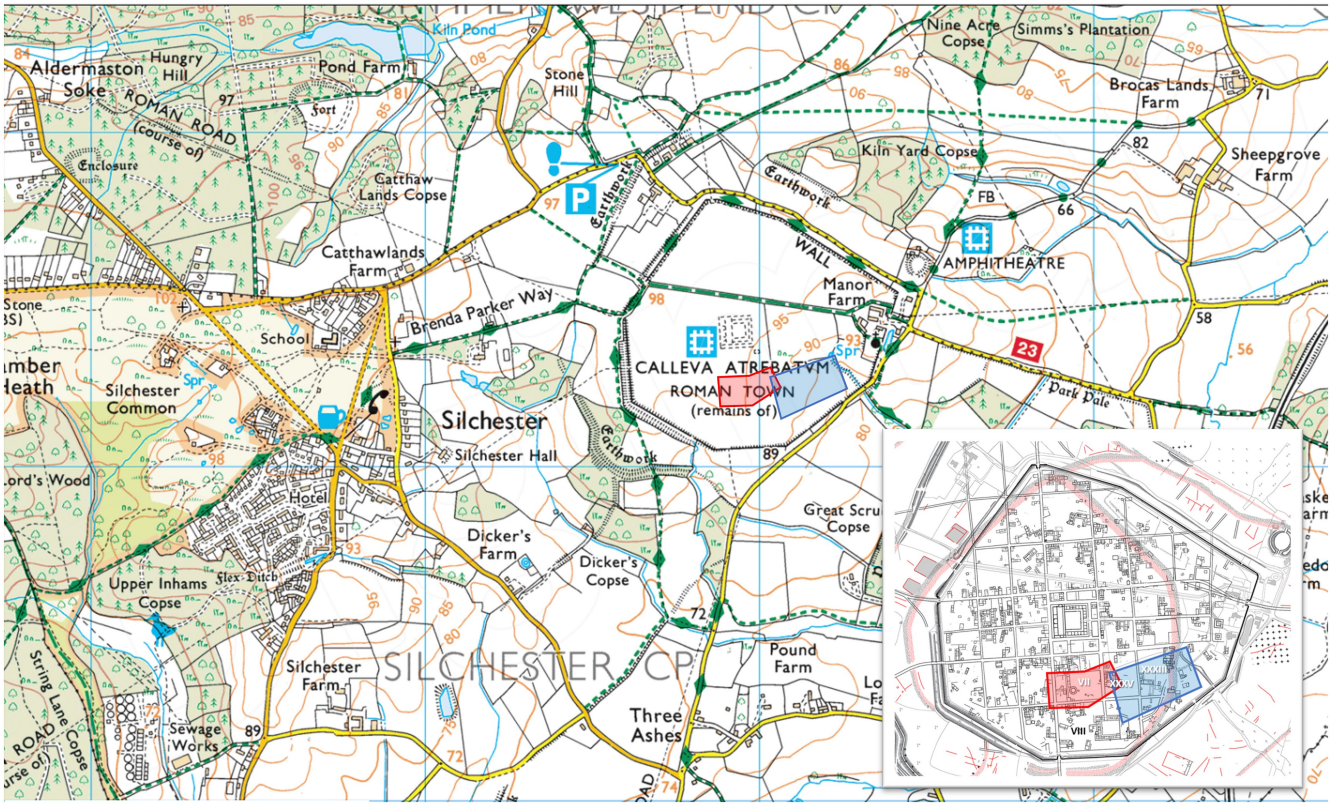

FIGURE 1 | Survey areas 1 and 2, outlined in red and blue, respectively, in the context of Silchester Roman Town and surrounding area (Digimap 2023). Inset: *Insulae* covered by the survey area.

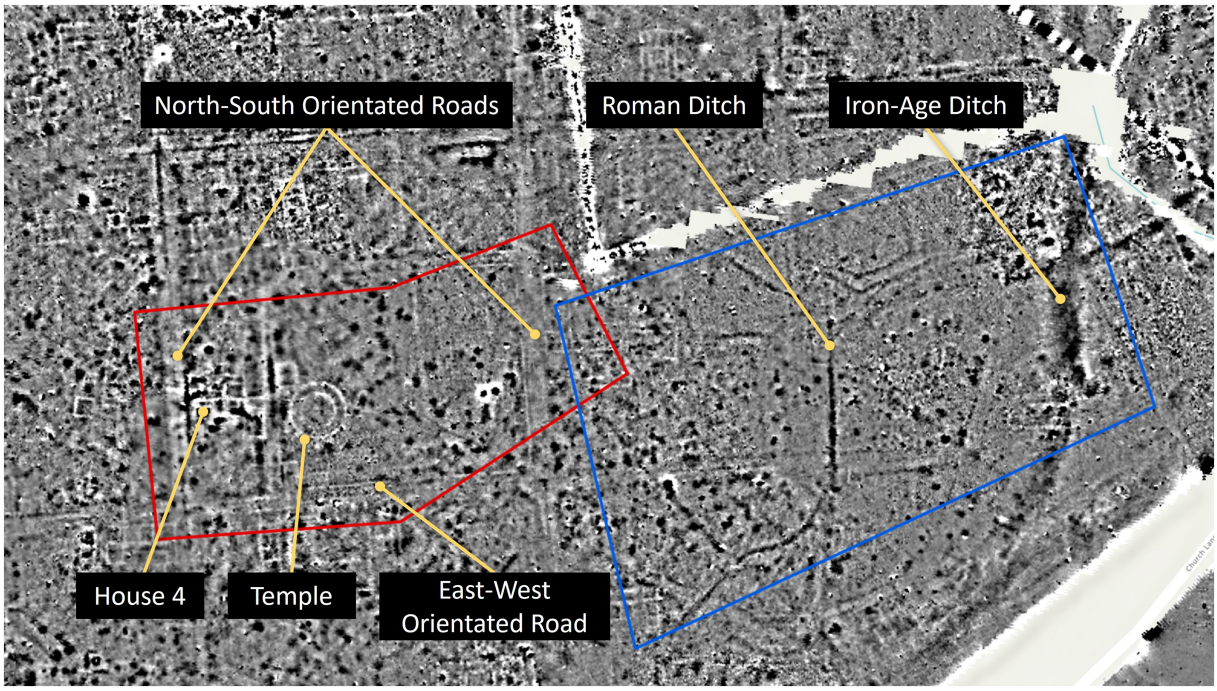

FIGURE 2 | Close-up view of the survey areas overlaying the fluxgate gradiometer data (+/− 7nT—black high to white low). The figure shows the targets present within Area A (outlined in red) and Area B (outlined in blue).

and sections of road in both north–south and east–west orientations. One of these roads is the major north–south road of the town, linking its North and South Gates (Fulford 2021). It is understood that House 4, as per other buildings on site, is predominantly of flint rubble construction with brick corner stones (Creighton and Fry 2016) and therefore of more typical construction to other buildings in the Town compared to the temple. It was identified as a good target for the gamma

radiation survey due to its shallow depth (approximately 30 cm below ground level) and its ability to generate a prominent magnetic anomaly in the extant Fluxgate Gradiometer data (Creighton and Fry 2016; Linford, Linford, and Payne 2019). The roads appear to be located at similar depths to the temple, as suggested by GPR data (Linford, Linford, and Payne 2019). The roads predominantly consist of compacted gravel extracted from quarries west of the Roman Town (Fulford 2021). The roads and temple targets were of particular interest to the authors. In the previous study by Robinson et al. (2022), the roads in *Insula* XXXIV failed to generate a measurable difference in gamma emissions relative to the surrounding substrate. The authors wished to explore whether these findings would be repeated for roads in a different area of the Silchester site or if different behaviours would be observed. The temple structure provided a novel target type of significant size to further test the efficacy of the Groundhog system.

3.2 | *Insulae* XXXIII

A larger ~1.4 ha area (Area 'B'), outlined in blue in Figure 2, was targeted in an adjacent space spanning *Insulae* XXXIII and XXXII (Figure 2). This site was selected due to the presence of two key features clearly present within the extant geophysics data: a large (Iron Age) defensive ditch running down the east of the survey area and a suspected Roman ditch for a drain or water supply (Figure 2). The Iron Age ditch was excavated in 2019 which demonstrated that it terminates at 4.8 m below the ground surface (Fulford et al. 2019). The ditch was selected for this study as it is analogous to targets clearly visible in the previous study: the ditch features associated with the temenos wall and the infilled clay pit. The Roman ditch offered a clear linear feature which turns into a long sweeping curve at the southern end of the survey area. It introduces a new target type to this research project and an opportunity to further test the efficacy of this technique.

It is noted that both study areas also contain other features such as large pits, wells, minor roads and structures that may also form targets of interest. However, due to their smaller size, they are less likely to generate significant contrasts in background radioactivity compared to the surrounding soil.

4 | Methodology

4.1 | Overview of Equipment Used

The use of a vehicle-mounted system facilitated the simultaneous operation of three Groundhog® gamma detector units. The Groundhog® units each contain a 76 mm × 76 mm sodium iodide (NaI) scintillation type gamma detector and spectrometer. The NaI detectors have an operating energy range of approximately 15–3000 keV. The units are linked to a mapping grade GPS unit and data logger in the form of an ultra-mobile personal computer (UMPC). One gamma spectrum measurement is recorded by the system every second, along with the corresponding positioning data.

With the deployment of three detectors in the vehicle-mounted system, it is possible to achieve the simultaneous collection of three gamma radiation measurements per second, with each gamma detector spaced 1 m apart. This contrasts significantly with the hand-held system's capacity for collecting one gamma radiation measurement per second, highlighting the enhanced efficiency afforded by the vehicle-mounted configuration.

4.2 | Site Surveys

Vehicle-mounted surveys were completed on 18 August 2022 and 16 May 2023. The second survey was originally unplanned and undertaken to fill in a substantial gap in the data on the eastern side of the survey area as a result of a GPS signal failure on the original survey (Area B) (Figure 4).

In advance of each deployment of the vehicle-mounted system, the three Groundhog® detector units were subject to full calibration, in accordance with Nuvia procedures. These annual calibration checks are essential to ensure that each unit is performing as expected and fit for purpose, thereby reducing the risk of introducing systematic errors. The Nuvia procedures are based on the National Physics Laboratory's Good Practice Guide 14 (Lee and Burgess 2014). The calibration process measured the gamma detectors' responses against background gamma radiation and a 5.72 kBq Cs-137 check source for a period of 600 s each. This confirmed that the gamma detectors were operating within acceptable ranges and therefore generating reliable data. The calibration checks confirmed that the detectors had an efficiency (i.e., the ratio of light pulses generated by the NaI crystal relative to the number of gamma rays emitted by the check source) of ~18 counts per second (cps) in the Cs-137 (662 keV) photopeak and net value of 3.17 cps which is well within the acceptable range of 2.93–3.24 cps. It was further confirmed that the detectors were operating with an energy resolution (i.e., the detector's ability to differentiate between energy peaks in a spectrum) of 7% at full width half maximum (FWHM) amplitude. Again, this was within the acceptable range of 6.50%–8.00%.

On the morning of each survey, the Groundhog® system was subject to additional equipment function checks. These were undertaken in accordance with Nuvia's internal Method Statement. Key activities included:

- Vehicle safety checks.
- Ensuring equipment has been subject to the necessary electrical safety checks.
- Visual checks of equipment and cables to ensure they are in good physical condition and that batteries have full charge.
- Functional checks of the Groundhog® system to ensure the GPS receiver and gamma radiation detectors were operating correctly. This included checking the responses of the detector unit, checking functionality of the necessary software tools, and that the GPS unit was receiving a sufficiently strong signal.

As the survey areas were located in a large open field, a detailed walk-round was not required. It could be seen that there were no obstructions or hazards that could impact on vehicle access.

It was however noted that one small area close to the Iron Age ditch was heavily rutted. While it was acknowledged that this would not impact on vehicle progress, suddenly dropping into a deep rut could trigger an 'excess speed' alarm on the UMPC. It could also potentially shock the NaI crystals of the detector units, leading to an erroneous measurement.

To facilitate the vehicle survey, the three gamma radiation detectors and GPS antenna were fixed in place using a mounting frame attached to the front of the Land Rover (Figure 3). The frame ensures that the detectors are securely positioned 1 metre apart at a consistent height of ~30 cm. The corners of the targeted survey areas, shown in Figure 2, were marked out with siting poles positioned using a Leica GS16 RTK GNSS unit.

The vehicle surveys were completed by driving around the perimeter of one of the predetermined survey areas and gradually working inwards towards the centre, following the tyre tracks of the previous circuit to avoid introducing gaps in the measurements. Several passes of the centre of each survey area were made due to the turning circle of the vehicle. A constant slow speed of approximately 1 m s^{-1} was maintained by placing the vehicle in first gear on a low transfer case setting ('low range'), thereby avoiding the need to apply acceleration. Maintaining this speed facilitated the collection of at least one gamma radiation measurement per square metre for each detector. This speed, combined with the simultaneous use of three detectors simultaneously enabled the collection of three radiation measurements every second, covering an area of three square metres. On completion of one survey area, the vehicle was relocated to the second predefined survey area (August 2022 survey only) and the process repeated.

4.3 | Data Processing

During the August 2022 and May 2023 surveys, gamma radiation and GPS measurements were automatically logged on the UMPC set up in the cab of the vehicle. At the end of each survey, these data were transferred to a stand-alone desktop computer for quality checks and preliminary processing.

As per the previous study, Microsoft Access (v. 16.0.14131.20278) was used to compile the data, with post-processing to improve the quality of location data undertaken in GrafNav (v. 8.3). RINEX data from the Hartley Wintney (HART) OS Reference Station was used for differential correction. Further quality checks, including checks on the completeness of the data, highlighted the significant gap in the August 2022 data within Area B. Later investigation showed that this affected an area of ~5500 m^2 (Figure 4), nearly a third of the eastern portion of the survey area, for which corresponding gamma data could not be plotted. These missing data informed the decision to resurvey the eastern side of the survey area to fill in this gap (Area B).

FIGURE 3 | View of the Nuvia survey vehicle, fitted with three Groundhog® Detectors and GPS system secured to the front. The detectors are spaced 1 m apart and positioned ~20 cm above ground level.

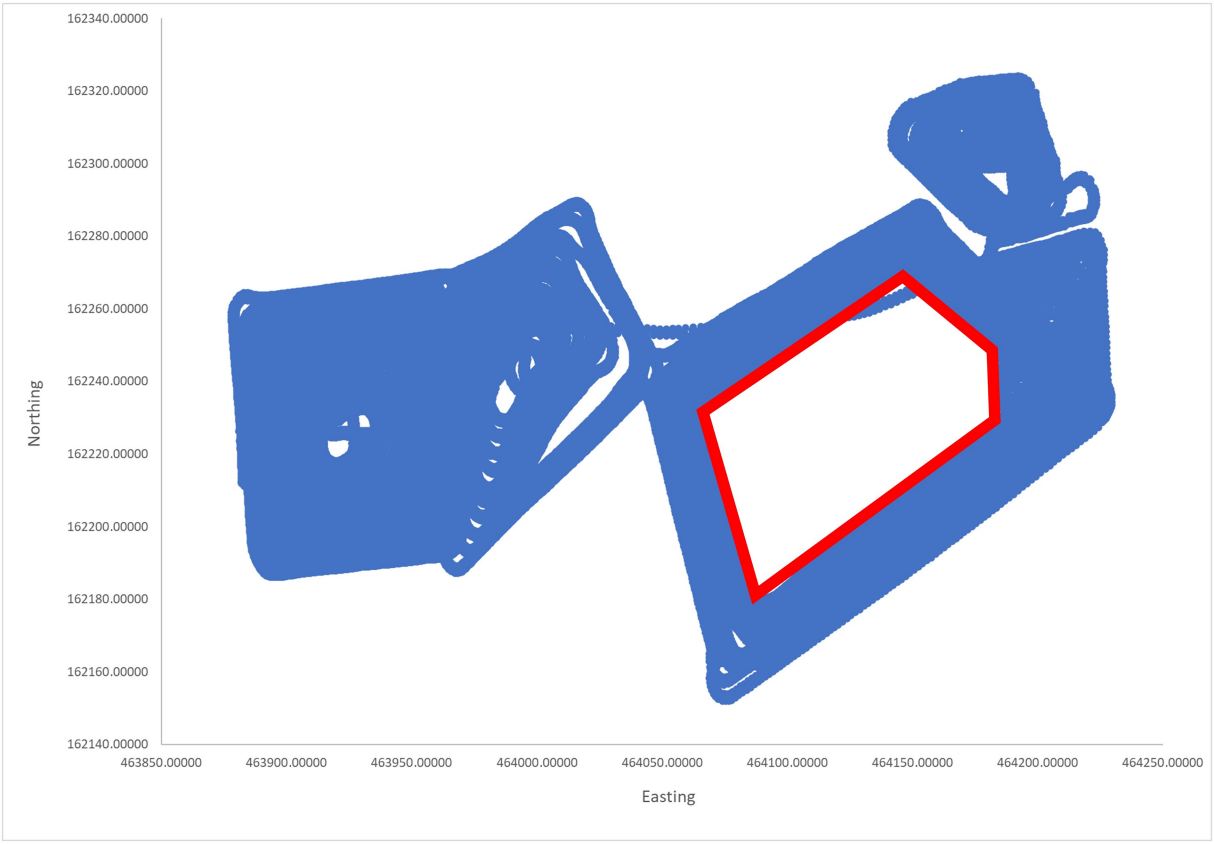

FIGURE 4 | Plot of the GPS/gamma radiation data points (blue) collected during the August 2022 survey, highlighting the area affected by missing GPS data (outlined in red).

With the exception of the missing GPS points, the remainder of the August 2022 and subsequent May 2023 positional data was excellent, achieving centimetre accuracy. Finally, quality checks also highlighted seven erroneous gamma radiation measurements in the May 2023 data. These values were an order of magnitude higher than the average readings in the dataset. The anomalous data points can be attributed to a physical shock to one of the NaI crystals in a detector unit, likely due to driving over the ruts or contacting tufts of long grass. It is considered improbable for measurements exceeding 3000 cps to occur naturally in an area with typical background radioactivity for the region. Notably, these elevated readings affected only one detector at a time. If there was a point source of elevated radioactivity in the ground, we would expect multiple detectors to record similarly high values. In consequence, these erroneous measurements were removed from the dataset.

Finally, both the August 2022 and corrected May 2023 datasets were exported as dBase database (.dbf) files for further processing.

The original strategy for processing the data was to combine the August 2022 and May 2023 datasets to create a single set of visualisations. This was accomplished using the Geoplot software tool (version 4). However, this was found to be non-viable. The data could not be integrated, with areas of overlaying measurements obscuring any potential anomalies present. As shown in Figure 5, the overlayed measurements actually created false positives, showing linear features that were attributable to vehicle movements.

To establish the cause of this incompatibility, gamma radiation measurements from two areas of overlap were samples (Figure 6) and subject to a two-tailed *t*-test, assuming unequal variances. The hypothesised mean difference was set at 0, assuming that there would be no significant difference in background gamma radiation measurements. A significance value of 0.05 was also set. As shown in Table 1, both sample areas confirm that the two datasets are significantly different, with p values of <0.05. After identifying a significant difference, the August 2022 data, which demonstrated a higher mean background gamma radiation value, were normalised against the May 2023 data. Multiple normalisation methods were applied, including subtracting the minimum value from each entry in the combined dataset and dividing by the range, dividing all values by the mean of the August 2022 and May 2023 mean values and dividing by mean and median values. None of these approaches addressed the problem. Consequently, a decision was made to process the August and May datasets separately, with resultant visualisations combined post-processing.

In the preliminary study by Robinson et al. (2022), gamma radiation data heatmaps were created exclusively in a bespoke add-on of ArcGIS, managed by Nuvia Limited. These heatmaps allowed the authors to identify anomalies that aligned with known archaeological features. However, for the purposes of this research project, a different software solution, Geoplot (version 4) was selected to plot the gamma data and create the visualisations. This choice not only enabled the exploration of alternative processing methods but also offered opportunities for enhancing image quality.

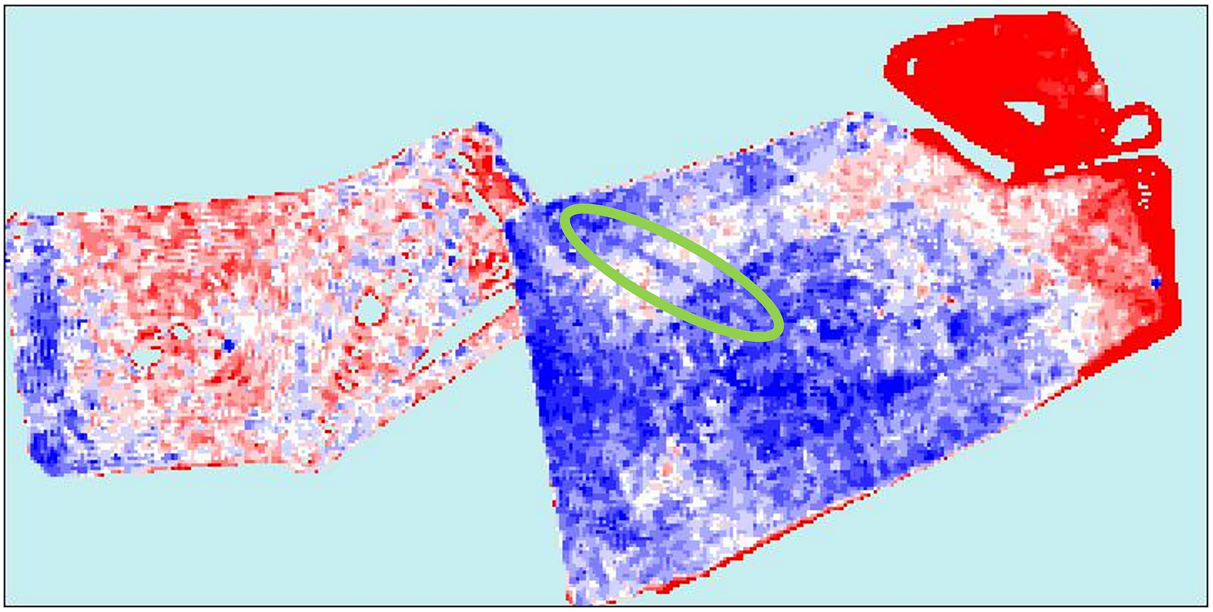

FIGURE 5 | Preliminary attempt at creating visualisations by combining the August 2022 and May 2023 datasets. This shows how the overlayed data are obscuring any anomalies and indeed creates false positives as highlighted in the green oval.

FIGURE 6 | Plot of the GPS/gamma radiation data points collected during the August 2022 and May 2023 surveys. Areas 1 and 2 denote where data were sampled for statistical analysis.

Further, this approach utilised a widely used software programme that does not require bespoke add-ons, improving accessibility.

Geoplot 4 offers a broad range of processing tools to enhance image quality. Work was therefore undertaken to explore which tools, or combination of tools, would generate the best quality visualisations. Different processing tools were applied to the total gamma counts per second recorded during both the August 2022 and May 2023 surveys. Care was taken to achieve an optimal balance between enhancing image quality to draw out features and excessively altering the output, reducing fidelity to the original datasets. Colour palette 09 (±2 standard deviations) was

TABLE 1 | Results from a two-tailed *t*-test for subsets of overlapping data from the August 2022 and May 2023 surveys as shown in Figure 6.

	Area 1		Area 2	
Parameters	**Aug 22**	**May 23**	**Aug 22**	**May 23**
Mean (cps)	225	189	237	199
Variance (cps)	310	239	359	259
Observations	3171	3264	2404	2950
Hypothesised mean difference	0		0	
df	6276		4727	
t stat	87.11		77.69	
$p(T \leq t)$ one-tailed	0.000		0.000	
t critical one-tailed	1.65		1.65	
$p(T \leq t)$ two-tailed	0.000		0.00	
t critical two-tailed	1.96		1.96	

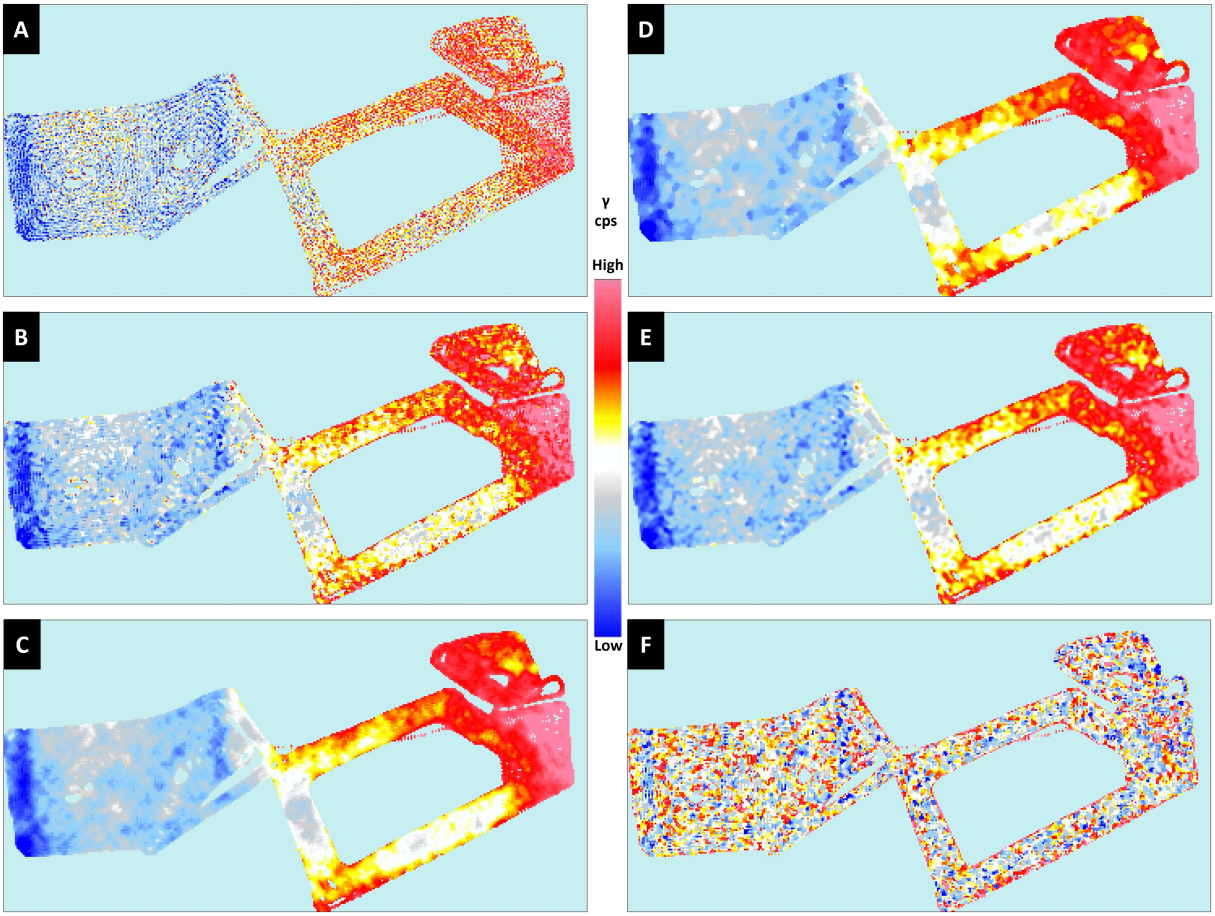

FIGURE 7 | Impact of different Geoplot processing tools on image quality for August 2022 total gamma counts (cps). The methods presented here are 'No Processing' (A), 'GPS Gap Fill' (B), Wallis Filter + GPS Gap Fill (C), Median Filter + GPS Gap Fill (D), Low Pass Filter + GPS Gap Fill (E) and High Pass Filter + GPS Gap Fill (F). The Wallis Filter + GPS Gap Fill (C) was identified as the preferred processing method.

found to be the most compatible with all processing methods to highlight the features of interest.

As a baseline, a single application of GPS Gap Fill was applied to the data. Subsequently, different data enhancement and smoothing filters (either a single application or combination of Wallis, median, low pass and high pass filters) were tested on the raw dataset, (Figure 7). The Wallis filter was found to optimise and enhance potential archaeological features within the dataset without overly smoothing the data.

Interrogation of the output images identified the combination of 'Wallis Filter + GPS Gap Fill' as the optimal method for processing the data. It created a smooth image capable of drawing out features of interest without excessive deviation from the raw data (Figures 7 and 9). This method was therefore applied to all subsequent processing.

Expanding on the data processing methods applied in the preliminary Silchester study (Robinson et al. 2022), the authors completed a more comprehensive analysis by investigating the specific impact of individual radionuclides on the observations from the 'total gamma counts' visualisations. Targeted radionuclides included both naturally occurring primordial radionuclides, namely, potassium-40, uranium-238 and thorium-232, and the anthropogenic caesium-137. Further, the authors examined energy windows that aggregated measurements falling below the caesium-137 energy range ('Below Window') and above it ('Above Window'). Targeting of these individual radionuclides was achieved by importing data from individual regions of interest into Geoplot. The ability to explore the impact of individual radionuclides has the exciting potential to offer additional interpretive value for more traditional geophysical surveys of archaeological deposits. By generating visualisations for each radionuclide, it may be possible to make inferences on the materials used on the construction of features identified as being of archaeological interest. For example, elevated concentrations of uranium and thorium may indicate the presence of granitic features, whereas concentrated areas of depleted radioactivity across all radionuclides may suggest features comprising sedimentary rock such as flint. More broadly, the behaviours of individual radionuclides may help characterise the geological history of the area, as evidenced in studies such as that undertaken by Kozhevnikov, Kharinsky, and Snopkov (2018).

As illustrated in Table 2, each radionuclide can be identified through its characteristic energy range. When a gamma radiation measurement is registered by a detector, it is assigned to the corresponding energy window. It is further noted that where radionuclides do not undergo decay through emission of gamma photons, a proxy daughter radionuclide that emits gamma photons is used, as shown in Table 2.

TABLE 2 | Regions of interest subject to interrogation via Geoplot.

Region of interest	Energy range (keV)
Total gamma	0–3000
Potassium (K) (via ^{40}K)	1400–1600
Uranium (U) (via ^{214}Bi)	1600–1900
Thorium (Th) (via ^{208}Tl)	2500–3000
Caesium (Cs) (via ^{137}Cs)	581–740
Below (^{137}Cs) window	0–530
Above (^{137}Cs) window	760–3000

Note: Each gamma ray photon emitted by a decaying radionuclide has a specific energy, typically measured in keV. This energy is unique to the source radionuclide (IAEA 2017). The energies of these gamma photons therefore act as a fingerprint, supporting the characterisation of radioactive material. Where there are multiple radionuclides present that emit gamma ray photons with similar energies, it may be difficult to differentiate between them, depending on the resolution of the detector used. For example, the radionuclides Pb-214, which emits gamma ray photons with energies of 295 and 351 keV, and Bi-214, which emits gamma ray photons of 609 and 665 keV (IAEA 2008), would fall in the Cs-137 region of interest of 581–740 keV, as shown in the above table for the Groundhog NaI gamma detectors.

5 | Results

The use of the vehicle-mounted Groundhog® system significantly increased the area that could be practically surveyed in a day. In the preliminary study by Robinson et al. (2022), where Groundhog® was deployed in a hand-held configuration, a total of ~16 000 m^2 was surveyed over a 2-day period. As shown in Table 3, approximately 23 500 m^2 was surveyed in a single day in August 2022, using the vehicle-mounted system. It is acknowledged that the efficiency of the hand-held surveys was impacted by the need to relocate between survey areas and the need to set up transect guides at each site. However, even once this inefficiency has been accounted for, it can be seen that the vehicle-mounted system significantly improves the scale of survey achievable. This supports the well-established findings from the commercial application of the Groundhog® system where it is known that a typical hand-held survey can cover hundreds to thousands of square metres (~15 000 readings per person/day) to tens of thousands of square metres per day (>50 000 readings per day).

Using the vehicle-mounted system also yielded a slight improvement in measurement density, increasing from a mean density of 1.3 measurements per square metre using the hand-held system (Robinson et al. 2022) to a mean of 2.2 measurements per square metre using the vehicle-mounted system as shown in Table 3. This improvement is attributable to the degree of overlap achieved during each pass of the Land Rover. This outlines the summary statistics for the August 2022 and May 2023 surveys, as well as those from the July 2019 survey of the Urban Area (Robinson et al. 2022), which is analogous in terms of target

TABLE 3 | Summary statistics for the August 2022 and May 2023 surveys shown against the July 2019 Urban Area survey for comparison.

Parameter	August 2022	May 2023	July 2019
Total area surveyed (m^2)	~23 500	~18 000	~4000
Total No. measurements	44 161	45 168	5255
Average No. readings/m^2	1.9	2.5	1.3
Minimum total gamma (cps)	132	124	163
Maximum total gamma (cps)	310	264	274
Mean total gamma (cps)	212	186	217
Standard deviation	24	16	16

Note: This highlights the improved survey density achieved by the vehicle-mounted system.
Source: July 2019 data are taken from Robinson et al. (2022).

types to the current survey areas. The total number of measurements recorded during each survey and minimum, maximum and mean readings collected are presented. Notably, the data from the May 2023 survey exhibit a closer resemblance to the July 2019 survey data than to the August 2023 data, the latter being collected during an extreme, high-temperature weather event. The two-tailed *t*-test applied to the datasets (Table 1) confirmed that the differences in the values observed for the August 2022 and May 2023 surveys are statistically significantly different.

5.1 | Total Gamma Emissions

Figure 7 presents the visualisations generated through the processing of total gamma counts recorded during the August 2022 survey. This figure reveals the impact of applying different processing tools on data quality.

The total gamma dataset from August 2022 identified two clear feature types within the survey area. These are clearly visible in both the raw data (Figure 7A) and processed data (Figure 7C–F). The first relates to the presence of linear features on the western extent of each dataset associated with Area A. There are two distinctive north–south aligned features and a less well-defined east–west feature running along the bottom of the area. These anomalies align very closely with known Roman roads clearly visible in the fluxgate gradiometer data (Figure 2). These linear features are present as areas of depleted radioactivity. The second feature of note is the clear transition from an area of generally low background radioactivity (~130–190 cps) in Area A, to a gradual increase in Area B, peaking at ~250–300 cps on the far eastern side of Area B. This observation is confirmed in the count rate distribution graph (Figure 8) which shows that gamma data from the August 2022 survey are not normally distributed. The chart demonstrates a bias towards lower counts per second, which will be influenced by the missing data from Area B where higher counts dominate. The transition from an area of lower background radioactivity in Area A to higher background radioactivity in Area B aligns with a historic field boundary running down the centre of the survey area. The localised area of elevated radioactivity in the far eastern side of Area B may be suggestive of a change in the hydrogeological conditions. These findings are explored further in Section 5.

It is recognised that none of the data processing methods were able to delineate the circular anomaly of the temple or the features of House 4, which were the other key features of interest in this area. This may be anticipated, given the comparatively less substantial structures of these features relative to the roads and considering the survey's spatial resolution. However, it is noteworthy that there is also an absence of any localised areas of either depleted or elevated levels of radioactivity that could be associated with these structures.

Visualisations generated for the May 2023 data that focussed solely on Area B are presented in Figure 9. As observed for the August figures, it is evident that various anomalies can be identified. Notably, two linear features are visible to varying degrees in all images: one running north to south and the other running east to west. These features, which appear as areas of depleted background radioactivity, again correspond closely to Roman roads as depicted in the existing fluxgate gradiometer data (Figure 2). Interestingly, the May 2023 visualisations reflect the same localised area of radioactivity present in the far east side of Area B, as observed in the August 2022 data. Again, this is reflected in the count rate distribution graph for May 2023 (Figure 8), which suggests data are not normally distributed, with a bias towards moderate count rates. It is noted that the area containing the highest concentrations of radioactivity on the far right of the images broadly aligns with the Iron Age Oppida bordering the area.

Again, not all features of interest visible in the Fluxgate Gradiometer data are present in the gamma radiation heat maps. In particular, there is no indication of the presence of the smaller ditch or culvert running through the centre of this survey area.

As might be expected, those filters capable of smoothing the data and drawing out weaker features have yielded the best results for both datasets. Notably, the Wallis (Figures 7C and 9C), median (Figures 7D and 9D) and low pass (Figures 7E and 9E)

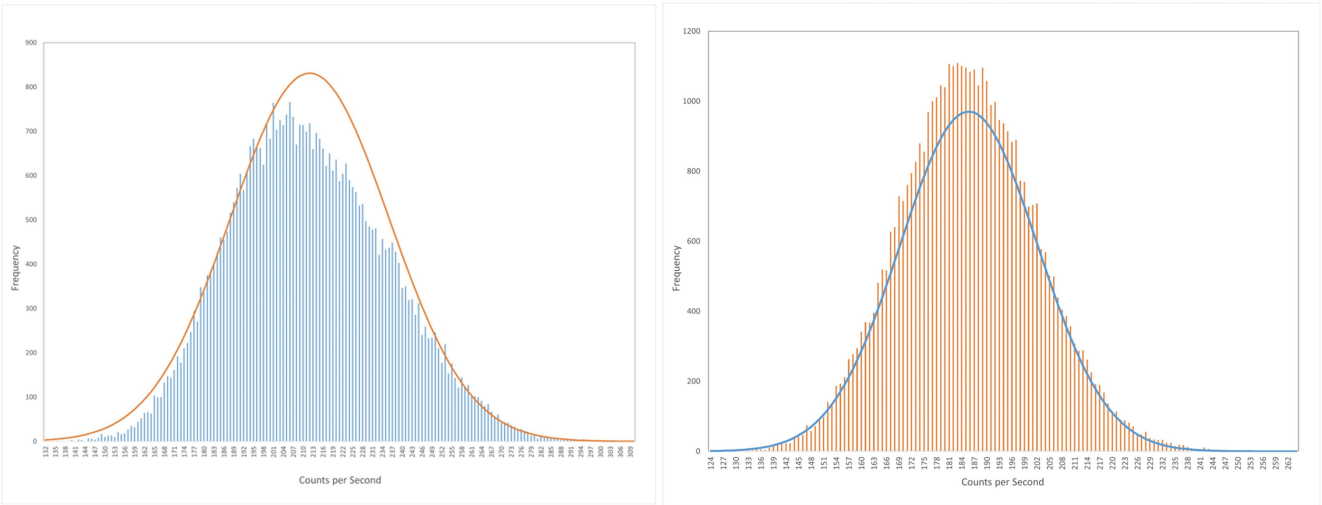

FIGURE 8 | Count rate distribution graphs for the August 2022 (left) and May 2023 (right) datasets. The August 2022 chart indicates that the background radioactivity is not normally distributed.

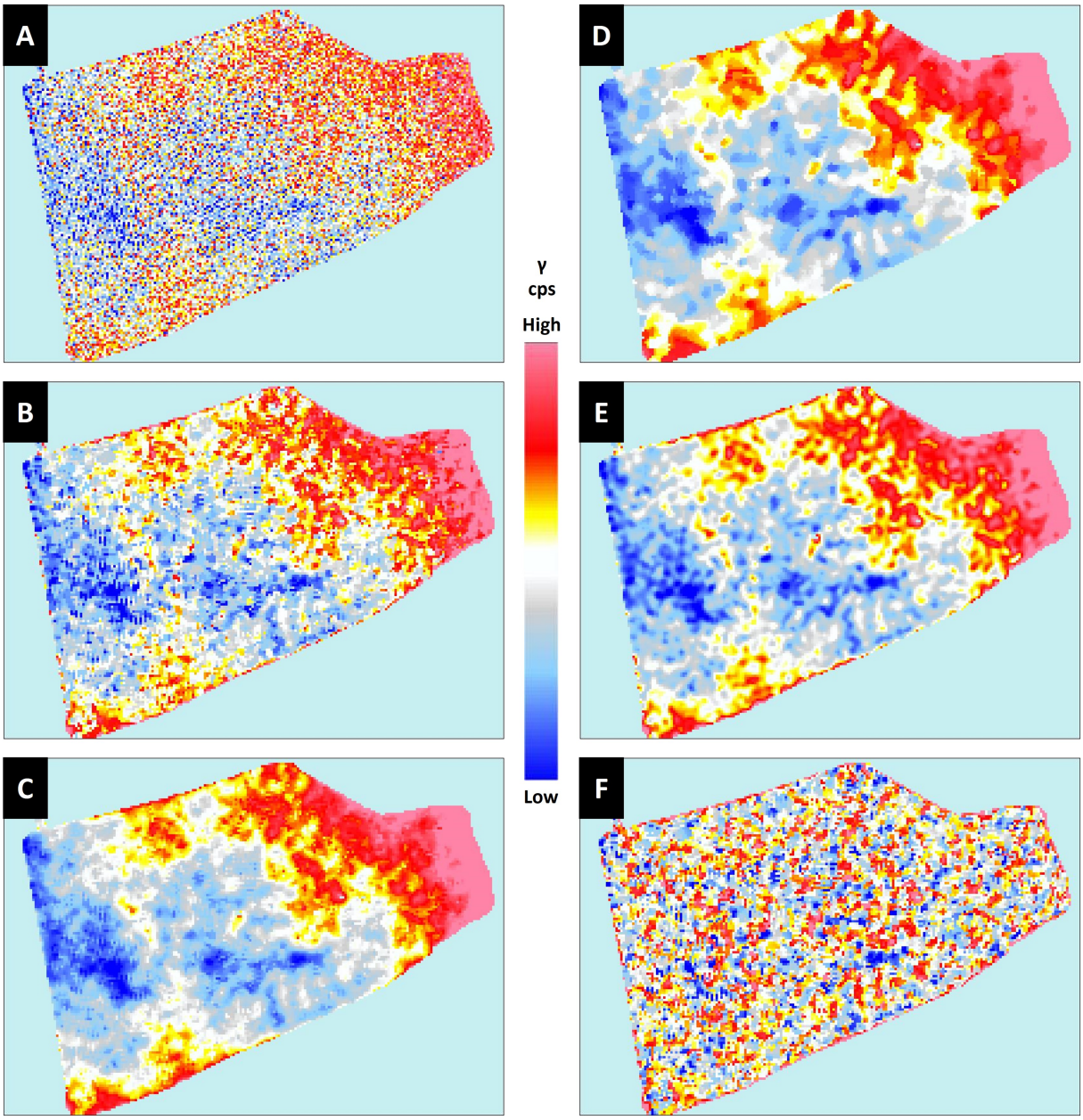

FIGURE 9 | Impact of different Geoplot processing tools on image quality for May 2023 total gamma counts (cps). The methods presented here are 'No Processing' (A), 'GPS Gap Fill' (B), Wallis Filter + GPS Gap Fill (C), Median Filter + GPS Gap Fill (D), Low Pass Filter + GPS Gap Fill (E) and High Pass Filter + GPS Gap Fill (F). The Wallis Filter + GPS Gap Fill (C) was identified as the preferred processing method.

filters have effectively reduced the 'noise' present and drawn out the linear features of the Roman roads without obscuring any detail. In contrast, the high pass filter that acts to remove low-frequency large-scale spatial detail (Geoscan 2014) has had a negative impact on image quality, obscuring features otherwise visible (Figures 7F and 9F).

5.2 | Understanding the Impact of Individual Radionuclides

Figures 10 and 11 provide visualisations for the contributions of individual radionuclides within the August 2022 and May 2023 surveys, respectively. Interestingly, visualisations for the potassium, thorium and caesium energy window data collected during the August 2022 survey (Figure 10A,C,D) reflect the findings of the total gamma count data; that count rates increase as you move eastwards across the survey areas.

For both the August 2022 and May 2023 surveys, the roads are faintly visible within the potassium energy window (Figures 10A and 11A), albeit to a lesser degree in the August 2022 figures. This may be due to the generally higher number of counts attributable to potassium in the May survey, making any shielding effects from the roads more prominent.

Uranium and thorium appear to be broadly uniformly distributed across the survey areas in both the August 2022

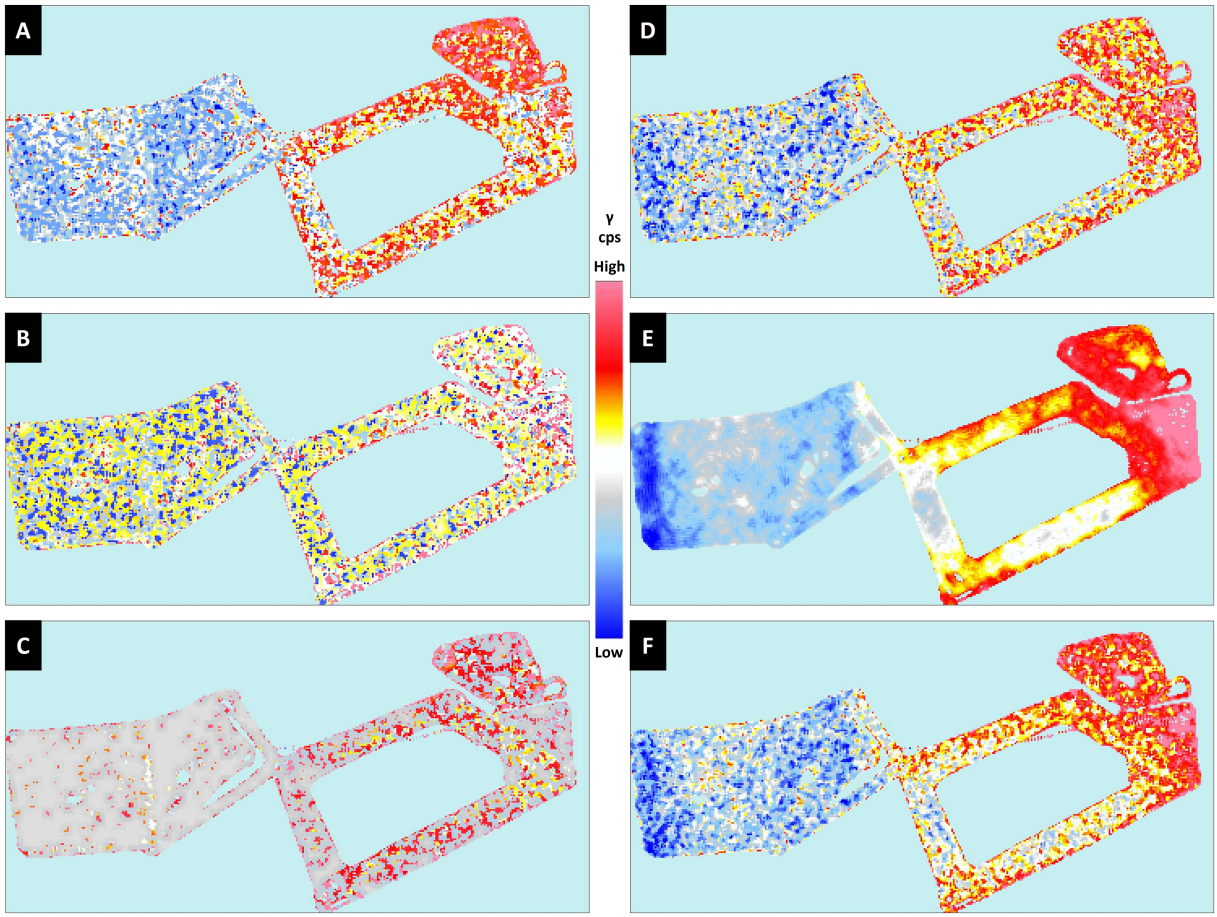

FIGURE 10 | Application of the Wallis Filter + GPS Gap Fill to the following regions of interest within the August 2022 dataset, as per Table 2: potassium (A), uranium (B), thorium (C), caesium (D), below window (E) and above window (F).

(Figure 10B,C) and May 2023 (Figure 11B,C), with no anomalies visible.

The linear features of the Roman roads are visible in the caesium data in the August 2022 visualisation (Figure 10D) and to a lesser extent in May 2023 (Figure 11D).

Data extracted from the 'below window' (Figures 10E and 11E) and 'above window' (Figure 11E,F) energy windows show that the contrast for the roads are most prominent here. The below window visualisations generate the highest quality images, even though it covers the smallest energy range (0–530 keV, relative to the 730–3000 keV emissions captured in the 'above window' dataset). This is in part attributable to the detector capturing gamma rays emitted from a range of naturally occurring radionuclides with similar energies including Pb-214 (with gamma photon energies of 52.2, 241.9, 295.2 and 351.9 keV), Ra-226 (with a gamma photon energy of 186.2 keV) and U-238 (with gamma photon energies of 49.5 and 113.5 keV) (IAEA 2008). Further, it is noted that NaI detectors of the dimensions used within the Groundhog® system (76 mm × 76 mm) are particularly efficient in this energy window (Mirion 2023).

Figures 10 and 11 suggest that potassium and caesium have the greatest impact on the visibility of any subsurface features. However, it is acknowledged that it is the total gamma counts that provide the best quality images overall. This is particularly well demonstrated in Figures 12 and 13 that show the combined August 2022 and May 2023 total gamma visualisations overlaying the Fluxgate Gradiometer data of Creighton and Fry 2016. These figures clearly show the alignment of the Roman roads between the two types of data. Figure 13 also provides an overlay of building outlines for further context. This confirms the absence of other key features such as the temple.

6 | Discussion

The surveys undertaken as part of this latest study underpin the findings of the preliminary investigation completed by Robinson et al. (2022). They have confirmed that portable gamma surveying methods can be effective at identifying features of archaeological interest. This is achieved by detecting measurable differences in concentrations of naturally occurring radioactive material present in or above archaeological targets and surrounding soil. However, as for the preliminary study, the August 2022 and May 2023 surveys have yielded mixed results.

Neither of the buildings or the thin linear Roman trench within *Insulae* VII, XXXV or XXXII were capable of generating

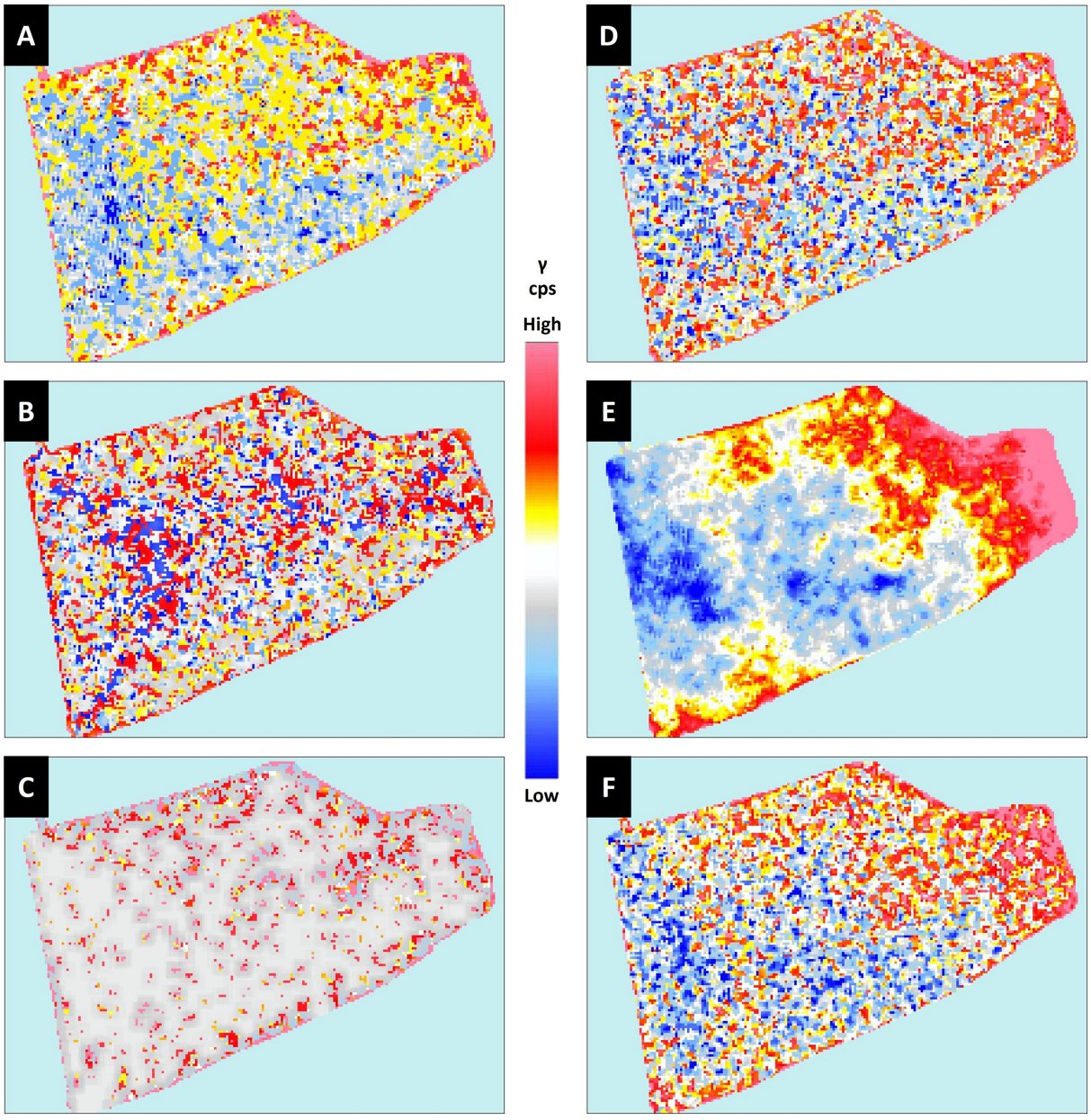

FIGURE 11 | Application of the Wallis Filter + GPS Gap Fill to the following regions of interest within the May 2023 dataset, as per Table 2: potassium (A), uranium (B), thorium (C), caesium (D), below window (E) and above window (F).

measurable contrasts in radioactivity as to be distinguished in the visualisations. This reflects the findings of the preliminary study which also failed to delineate the outlines of known buildings. It is possible that this is attributable to the less robust structures of these buildings, reducing their ability to create a sufficient contrast in background gamma radiation measurements. This effect may be exacerbated by the resolution of the surveys. Alternatively, it is possible that the materials of construction have a similar gamma radionuclide composition to the surrounding soil than observed for the roads. While the difficulty in clearly delineating these less substantial features may be expected for these reasons, it is interesting that there are no general areas of localised increased or decreased counts attributable to the disturbance caused by this past activity. Further work is therefore planned to explore this finding through collection and analysis of samples of building materials and soils.

A welcome finding of this latest study was the ability to delineate road structures. This was not achieved in the preliminary study. In both the August 2022 and May 2023 data, roads appear as areas of low background radioactivity. Particular attention is drawn to the roads visible in the August 2022 'total gamma' visualisations (Figure 7). In all iterations of this image, Silchester's primary north–south road, visible on the left-hand side of each image, is the most prominently featured, followed by a secondary north–south road to the right. In contrast, the east–west road is showing a very weak contrast and is incomplete in the gamma data. This variability is absent in the Fluxgate Gradiometer data shown in Figure 2. It is suggested that variations in the observed gamma radionuclide content of the roads may be indicative of varying thicknesses of road material which possesses a lower concentration of radioactive material relative to the surrounding soil. Consequently, it shields the gamma radiation emitted from

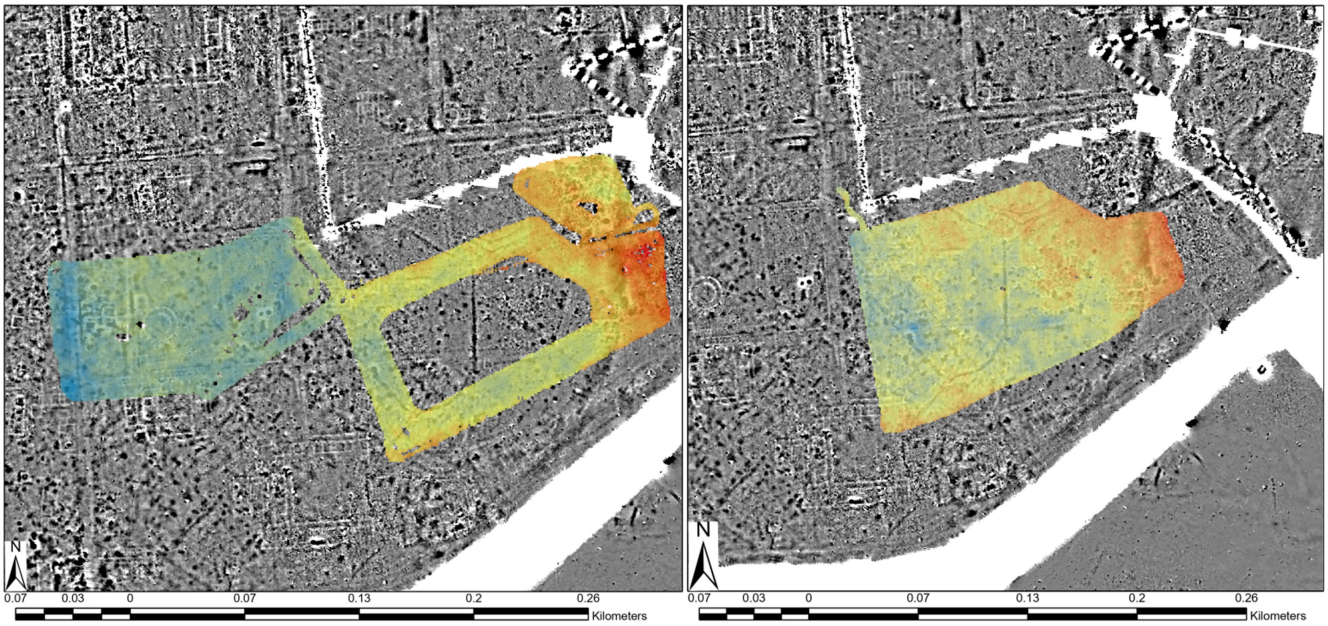

FIGURE 12 | August 2022 (left) and May 2023 (right) Geoplot-processed data overlayed on existing Fluxgate Gradiometer data, demonstrating the alignment of observed anomalies. Gamma radiation data has been set at 25% transparency to reveal underlying anomalies.
Source: Fluxgate Gradiometer Data from Creighton and Fry (2016).

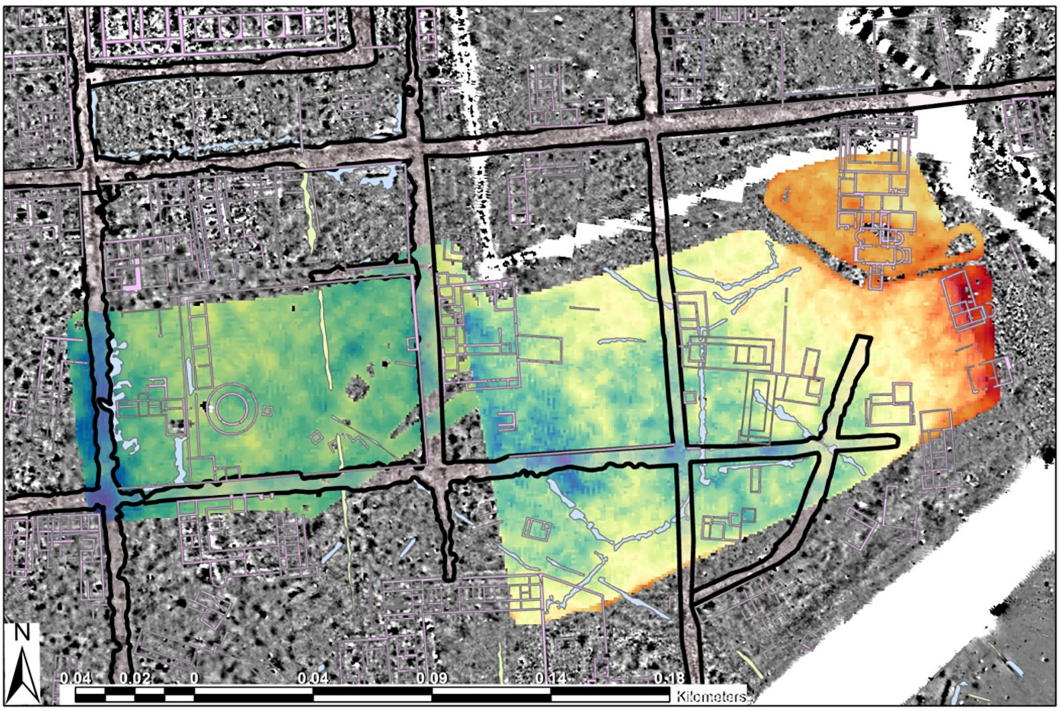

FIGURE 13 | Combined August 2022 and May 2023 Geoplot-processed data overlayed on existing Fluxgate Gradiometer data, with previously mapped features overlayed demonstrating alignment of the anomalies in the gamma radiation data with known features. Overlayed data include the Antiquaries Great Plan (pink lines), the Fluxgate Gradiometer interpretation of the roads (black outlines), positive linear features in the Fluxgate Gradiometer data (blue lines) and historic field boundary from 1759 (red dotted line).

the underlaying soil to a different extent. This is supported by the work of Fulford, Clarke, and Pankhurst (2024) who note that the main north–south road is a substantial structure, measuring up to 7.6 m in width and approximately 1 m in thickness. In contrast, the east–west road is up to 6 m wide and 0.85 m thick (Fulford, Clarke, and Pankhurst 2024). Another factor contributing to the observed variations in the gamma radionuclide content of the roads is the extent of material consolidation. Previous excavations revealed that the materials comprising the main north–south road had become cemented together, presenting a

more solid mass (M. Fulford, personal communication). This increased consolidation, combined with the increased thickness in the road material, may have enhanced the shielding effect. The cause of this cementation process is unknown but may be attributable to the heavy use of this street and its accommodation of carts carrying substantial loads of up to 500 kg (M. Fulford, personal communication). This discovery suggests that portable gamma radiation data collected as part of an archaeological investigation could aid interpretation of traditional geophysical survey outputs, enhancing the value of other nonintrusive surveys. This is particularly relevant when it is recognised that in the fluxgate gradiometer dataset, the clear delineation of the roads is largely attributable to the accompanying roadside ditches, rather than the deposition of the flint and gravel itself.

In addition to the linear anomalies attributable to the roads, another feature of interest is the transition from an area of lower radioactivity in Area A to higher activity in Area B. This is clearly visible in the August 2022 survey data (Figure 7). The point of transition, where Areas A and B connect, aligns closely with a historic field boundary visible in a 1759 plan of Silchester, as depicted in Figure 13. This boundary may be indicative of differing land uses that have caused changes in soil chemistry or composition, which in turn has influenced the adsorption/retention of radionuclides. This field boundary may also be visible in the gamma radiation data. In the May 2023 survey, there is a north–south aligned linear feature, present as an area of depleted radioactivity, running along the left-hand edge of the survey area (Figure 9). Specifically, this appears to be attributable to localised reductions in concentrations of potassium, thorium and caesium (Figure 11). As shown in Figure 13, this linear anomaly does not align with any of the Roman roads but does closely follow the 1759 boundary. It is noted that this boundary is not present in the later 1841 tithe map for the area (Hampshire Archives 2023a). However, the accompanying Tithe Award identifies the area within which the gamma radiation survey data sits as the 'Watch Field and the Nine Acres' (Hampshire Archives 2023b). The area to the right of the 1759 field boundary is approximately nine acres in size. This further suggests that the two sides of this field remained distinct for an extended period, even though the physical field boundary was no longer present.

The area containing the highest levels of radioactivity, running along the right-hand edge of Area B is present in both the August 2022 and May 2023 data. This aligns closely with the location of the Iron Age ditch and an area prone to waterlogging.

The waterlogged area aligning with the Iron Age ditch is expected to have a different chemistry to the adjacent soil. This difference can influence the behaviour of naturally occurring radionuclides present. For example, uranium in soils is commonly found as a mobile form of UO_2 in its U (VI), particularly in slightly basic to acidic soils (Smedley and Kinniburgh 2023). However, under strongly reducing conditions, the uranium can be reduced to its U (IV) state, leading to its precipitation as an immobile form of UO_2 or otherwise become sorbed onto the surface of soil particles (Smedley and Kinniburgh 2023), thereby increasing uranium concentrations in the soil. The waterlogged area at Silchester could provide such conditions. Further, this area is rich in clay deposits, contributing to waterlogging. The Iron Age defensive ditch is cut into London Clay, eventually becoming infilled with a mixture of clays and anthropogenic deposits, including brick and organic materials (M. Fulford, personal communication). The location of the elevated radioactivity coincides with an area where the gravel capping over the London Clay had been eroded away (M. Fulford, personal communication). The presence of these clay deposits increases the chance of accumulating radionuclides such as caesium-137 which adsorbs strongly to clay particles (Ritchie 1998). The authors intend to further characterise this area as part of ongoing research to gain a better understanding of the geochemical properties of the area and how these properties vary across the site profile.

The equipment failure during the August 2022 survey and requirement to resurvey the eastern side of the site provided an additional opportunity to explore the impact of changing soil moisture content on the effectiveness of portable gamma surveying, recognising the potential for shielding from interstitial water. The August 2022 survey was conducted in what may be considered optimal ground conditions, minimal soil moisture following an extended period of very low rainfall and high temperatures. Indeed, evidence suggests that this was the fourth driest summer on record (McCarthy 2022). This contrasts with the meteorological conditions in May 2023, where the first half of the month saw rainfall levels exceed the mean value for the period 1991–2020 for the same month (Met Office 2023). As a result, soil moisture content and therefore potential for increased gamma radiation shielding was much higher in May. It might therefore be expected that the May 2023 survey would yield lower quality results. However, as seen in Figures 7 and 9, groundwater in this case does not appear to have a significant impact on data quality, with road structures clearly visible in both conditions. However, it is noted that this survey has resulted in generally lower levels of radioactivity recorded overall, which is expected to be attributable to a degree of shielding by interstitial water. It is recognised that this result in isolation is insufficient to draw any meaningful conclusions on this aspect, and therefore, further research is required to fully understand the impact of groundwater conditions on gamma survey data quality in archaeological applications.

In addition to the aspects identified for further investigation already discussed, it is acknowledged that there are still multiple other areas that require further exploration. This includes conducting surveys at different locations to explore the impact of varying geologies, testing the responses of different target types (e.g., considering materials of construction, size and burial depths) and the completion of surveys in more controlled conditions to facilitate better control of individual variables.

7 | Conclusions

This study has provided a valuable opportunity to further challenge the viability of portable gamma surveying as a contributory tool for nonintrusive archaeological prospection. This has been achieved by:

1. Testing the replicability of the technique by surveying areas containing analogous target types to the preliminary study completed by the authors;
2. Testing scalability of the technique by applying a vehicle-mounted Groundhog® system; and
3. Exploring alternative data processing methods to improve the quality of the visualisations used to identify anomalies that could be attributable to archaeological features of interest.

Completion of this latest suite of gamma radiation surveys has confirmed that the method can be successfully scaled to encompass a much larger survey area without compromising data quality. As per the preliminary investigation, the latest surveys have yielded mixed results with the Groundhog® system successfully delineating some known archaeological features such as Roman roads, while failing to detect others such as buildings. Interestingly, the types of targets detectable have not been consistent between the two studies. In the preliminary study, roads and buildings could not be identified whereas ditches created clear anomalies. In this latest study, roads were consistently capable of generating anomalies within the gamma radiation data, whereas this was less successful for the ditches. Where the area of elevated radioactivity aligns with the Iron Age ditch, there is some uncertainty as to whether the anomaly can be attributed to the ditch itself or if it is indicative of ground disturbance associated with past excavations.

The strength of the anomalies associated with each road may indicate variations in either the depth of road material or construction materials, suggesting that gamma radiation data could aid interpretation of other geophysical survey outputs. This strengthens the argument that portable gamma surveying can add value to nonintrusive archaeological investigations.

There is notable uncertainty regarding the causes of some of the observed outcomes. This uncertainty relates to the absence of measurable differences in gamma radiation levels present in/over archaeological targets (identified as being strong candidates) and surrounding soils and the discrepancy in the types of targets discernible in the preliminary and current investigations. Consequently, additional investigations and research is imperative if these uncertainties are to be adequately addressed. This will be achieved through the direct radiochemical analysis of samples of soil and target material and surveying of new archaeological sites.

The use of an alternative software tool, Geoplot, has provided a valuable opportunity to apply different processing tools to enhance the quality of visualisations generated. This was successful, with the Wallis filter, in particular, being able to draw out features of interest without deviating too far from the raw data.

The ability to investigate the influence of individual radionuclides on the results observed has also produced interesting insight and may aid interpretation of the total gamma visualisations. This includes identifying areas of ground disturbance indicative of previous excavation works. It is believed that this area also warrants further explanation.

Overall, this latest study has proven to be a successful progression of the preliminary investigation confirming that portable gamma surveying methods can identify archaeological features of interest. However, further work is now required to better understand what types of features are most amenable to this technique and how it can be most effectively applied.

Acknowledgements

This unique investigation was possible thanks to Nuvia Limited who provided access to the Groundhog® fusion vehicle-mounted system and supporting software tools. The authors wish to express their thanks and gratitude to Ben Kolosowski and the University of Reading for permitting and facilitating access to the Silchester site and to Anthony Sweeney for helping to set up the equipment at Silchester.

Conflicts of Interest

The authors declare no conflicts of interest.

Data Availability Statement

The data that support the findings of this study are available from the corresponding author upon reasonable request.

References

Aliyev, C. 2004. "NORM in Building Materials." In *IAEA (2004) Naturally Occurring Radioactive Materials (NORM IV): Proceedings of an International Conference Held in Szczyrk Poland, 17–21 May 2004, IAEA-TECDOC-1472*. Vienna Austria: IAEA.

Creighton, J., and Fry, R. 2016. *Silchester: Changing Visions of a Roman Town: Integrating Geophysics and Archaeology: The Results of the Silchester Mapping Project, 2005-10*, Britannia Monograph Series; vol. 28, Hampshire, UK: Society for the Promotion of Roman Studies. ISBN: 9780907764427.

Cuenca-Garcia, C. 2018. "Soil Geochemical Methods in Archaeogeophysics: Exploring a Combined Approach at Sites in Scotland." *Archaeological Prospection* 26, no. 1: 57–72. https://doi.org/10.1002/arp.1723.

Digimap. 2023. Silchester Overview, PDF Map, Scale 1:10000, Projection: British National Grid (EPSG:27700), OS Master Map, March 2023, Ordnance Survey Using Digimap Ordnance Survey Collection. Created 22 October 2023. https://digimap.edina.ac.uk/

Fulford, M. 2021. *Silchester Revealed: The Iron Age and Roman Town of Calleva*. Havertown: Windgather Press. ISBN: 9781911188865.

Fulford, M., A. Clarke, J. Eaton, et al. 2019. *Silchester Roman Town: The Baths 2019*. Reading, UK: Department of Archaeology, University of Reading.

Fulford, M., A. Clarke, and N. Pankhurst. 2024. *Silchester Insula IX. Oppidum to Roman City, c. A.D. 85-125/50. Final Report on the Excavations 1997–2014*, London, Society for the Promotion of Roman Studies. Britannia Monograph 37.

Gaffney, C., and J. Gater. 2011. *Revealing the Buried Past: Geophysics for Archaeologists*. Gloucestershire, UK: Tempus Publishing Ltd.

Geoscan. 2014. Geoplot Version 3.0 for Windows: Datasheet Issue 13, GPW300_13 PPX2, June 2014. Accessed October 2023. Created June 2014, http://www.geoscan-research.co.uk/Geoplot3_v13_Data_Sheet.pdf.

Hampshire Archives. 2023a. Plan of the Parish of Silchester in the County of Hants 1841. Accessed October 2023.

Hampshire Archives. 2023b. Apportionment of the Rent-Charge in Lieu of Tithes in the Parish of Silchester in the County of Southampton (sic), Published by Routledge London 1841. Accessed October 2023.

IAEA. 2003. *Extent of Environmental Contamination by Naturally Occurring Radioactive Material (NORM) and Technological Options for Mitigation*, Technical Report Series No. 419, International Atomic Energy Agency, Vienna.

IAEA. 2008. *Handbook of Nuclear Data for Safeguards: Database Extensions, INDC (NDS)534*. Vienna: International Atomic Energy Agency.

IAEA. 2017. *In Situ Analytical Characterization of Contaminated Sites Using Nuclear Spectrometry Techniques, Review of Methodologies and Measurements*, IAEA Analytical Quality in Nuclear Applications Series No. 49, International Atomic Energy Agency, Vienna.

IAEA. 2023. Radiation in Everyday Life. Vienna: International Atomic Energy Agency (IAEA). Accessed 21 January 2023. https://www.iaea.org/Publications/Factsheets/English/radlife.

Jordan, D. 2009. "How Effective Is Geophysical Survey? A Regional Review." *Archaeological Prospection* 16: 77–90. https://doi.org/10.1002/arp.348.

Kozhevnikov, N. O., A. V. Kharinsky, and S. V. Snopkov. 2018. "Geophysical Prospection and Archaeological Excavation of Ancient Iron Smelting Sites in the Barun-Khal Valley on the Western Shore of Lake Baikal (Olkhon Region, Siberia)." *Archaeological Prospection* 2018: 1–17. https://doi.org/10.1002/arp.1727.

Lee, C. J., and P. H. Burgess. 2014. *Good Practice Guide 14, The Examination, Testing and Calibration of Portable Radiation Protection Instruments*. NPL, Middlesex, UK: National Physics Laboratory (NPL) Issue 2, First Issued—1999, Updated—2014.

Linford, N., P. Linford, and A. Payne. 2019. *Silchester Roman Town Hampshire: Report on Geophysical Surveys June 2009, March 2014 and July 2015*, Research Report No. 85-2019. Portsmouth, UK: Historic England, ISSN: 2059-4453.

Lovelock, J. 2000. *Gaia: A New Look at Life on Earth*. Oxford, UK: Oxford University Press. ISBN: 9780192862181.

McCarthy, M. 2022. "Guest Post: A Met Office Review of the UK's Record-Breaking Summer in 2022." *Carbon Brief*. Accessed 17 August 2023 Last Updated: 28/09/2022. https://www.carbonbrief.org/guest-post-a-met-office-review-of-the-uks-record-breaking-summer-in-2022/.

Met Office. 2023. May 2023 Monthly Weather Report. Accessed October 2023. Last Updated: May 2023. https://www.metoffice.gov.uk/binaries/content/assets/metofficegovuk/pdf/weather/learn-about/uk-past-events/summaries/mwr_2023_05_for_print.pdf.

Milsom, J., and A. Eriksen. 2011. *The Geological Field Guide Series: Field Geophysics*. 4th ed. Sussex, UK: Wiley-Blackwell.

Mirion. 2023. *Gamma and X-Ray Detection*. Harwell, UK: Mirion Technologies. Accessed 10 December 2023, https://www.mirion.com/discover/knowledge-hub/articles/education/nuclear-measurement-fundamental-principle-gamma-and-x-ray-detection.

Porcelli, F., L. Sambuelli, C. Comina, et al. 2020. "Integrated Geophysics and Geomatics Surveys in the Valley of the Kings." *Sensors (Basel, Switzerland)* 20, no. 6: 1552. https://doi.org/10.3390/s20061552.

Ritchie, J. C. 1998. "^{137}Cs Use in Estimating Soil Erosion—30 Years of Research." In *IAEA (1998) Use of ^{137}Cs in the Study of Soil Erosion and Sedimentation, IAEA-TECDOC-1020*. Vienna: International Atomic Energy Agency.

Robinson, V., R. Clark, S. Black, R. Fry, and H. Beddow. 2022. "Portable Gamma Ray Spectrometry for Archaeological Prospection: A Preliminary Investigation at Silchester Roman Town." *Archaeological Prospection* 29, no. 3: 353–367. https://doi.org/10.1002/arp.1859.

Ruffell, A., and J. McKinley. 2008. *Geoforensics*. New Jersey, USA: Wiley-Blackwell.

Simon, F. X., T. Kalayci, J. C. Donati, C. Cuenca-García, M. Manataki, and A. Sarris. 2015. "How Efficient Is an Integrative Approach in Archaeological Geophysics? Comparative Case Studies From Neolithic Settlements in Thessaly (Central Greece)." *Near Surface Geophysics* 13, no. 6: 633–643. https://doi.org/10.3997/1873-0604.2015041.

Smedley, P. L., and D. G. Kinniburgh. 2023. "Uranium in Natural Waters and the Environment: Distribution, Speciation and Impact." *Applied Geochemistry* 148: 105534. https://doi.org/10.1016/j.apgeochem.2022.105534.

Ward, J. 1911. *Romano-British Buildings and Earthworks, Chapter 10, Volume 24 of Antiquary's Books*. North Yorkshire, UK: Methuen & Company Limited. ISBN: 0598613269, 9780598613264.

Wynn, J. C. 1986. "A Review of Geophysical Methods in Archaeology." *Archaeology* 1, no. 3: 245–257. https://doi.org/10.1002/gea/3340010302.